atmosphere

MDPI

Article

Morphological and Mineralogical Characteristics of Atmospheric Microparticles and Chemical Pollution of Street Dust in the Moscow Region

Varvara M. Kolesnikova [1,*], Olga A. Salimgareeva [1], Dmitry V. Ladonin [1], Victoria Y. Vertyankina [2] and Anna S. Shelegina [1]

[1] Faculty of Soil Science, Lomonosov Moscow State University, 119992 Moscow, Russia
[2] Yu. A. Izrael Institute of Global Climate and Ecology, 107258 Moscow, Russia
* Correspondence: kolesnikovavm@my.msu.ru; Tel.: +7-4959393641

Abstract: Comprehensive morphological and mineralogical studies of atmospheric microparticles sampled on the roof of the museum complex and near roads in the town of Istra, Moscow region, have been carried out. Morphological research at different hierarchical levels revealed the multicomponent composition of microparticles and made it possible to identify the most characteristic groups of microparticles of natural and anthropogenic origin. The composition of the studied atmospheric microparticles is dominated by mineral grains of quartz and feldspars; biotite and calcite are singly noted, which reflects the ecological and geographical conditions of their formation, namely the Central Russian mineralogical province. A small share of technogenic particles in the composition of aerosol fallout indicates a low level of technogenic load and a favorable environmental situation in the study area, largely due to the protective functions of the forest park zone. The results of determining the material composition and calculating the enrichment factors also indicate a low level of technogenic impact on the natural environment.

Keywords: dust; dust transport; air pollutants; mineralogical analysis; technogenic microparticles; biological aerosols

Citation: Kolesnikova, V.M.; Salimgareeva, O.A.; Ladonin, D.V.; Vertyankina, V.Y.; Shelegina, A.S. Morphological and Mineralogical Characteristics of Atmospheric Microparticles and Chemical Pollution of Street Dust in the Moscow Region. *Atmosphere* **2023**, *14*, 403. https://doi.org/10.3390/atmos14020403

Academic Editor: Longyi Shao

Received: 31 January 2023
Revised: 16 February 2023
Accepted: 17 February 2023
Published: 19 February 2023

1. Introduction

The transfer of atmospheric microparticles is thought to cause numerous environmental issues, from climate change to a negative impact on human life and health; works of many authors are devoted to various aspects of the problem [1–4]. As a two-phase system—aerosol dust consists of a dispersion medium (air) and a dispersed phase—solid and liquid particles suspended in the air and differing in their physicochemical composition and genesis. Atmospheric dust affects the air temperature and the earth's surface diversely: the daytime decrease in the temperature of the earth's surface and the nighttime slight increase [1]. Owing to sand and dust storms, a huge amount of sand and dust following the strong wind rises from the earth's surface and is carried into the atmosphere. On the back of sandstorms, formidable quantities of living cells of microorganisms, pollen, endotoxins, mycotoxins, heavy metals and other substances are migrated annually [4–6]. Dust is capable of residing in all layers of the Earth's atmosphere and, depending on its size and genesis, does not settle for a long time to the surface and is transported over considerable distances.

Apart from vehicles, the main sources to form technogenic atmospheric microparticles in cities are enterprises of light and heavy industry, whose work is associated with such industrial processes as combustion, roasting, and chemical reactions.

Microparticles that settle on impermeable urban surfaces are commonly referred to as urban street dust [7]. The urban environment is a hotbed of air pollution ([4,8–14], etc.), the health risks of toxic heavy metals in road dust have been studied [14]. It has been

established that dust aerosol content in the air of cities exceeding the permissible levels affects negatively human health, both chemistry and dust particles size involved [2]. Monitoring of atmospheric air pollution by fine suspended particles (particulate matter—PM) is carried out in megapolis and areas of high technogenic load. The content of particles in the air with dimensions < 2.5 microns and <10 microns (PM2.5 and PM10, respectively), which have the most pronounced negative impact on human health, is monitored. Micro- (2.5–0.1 microns) and ultrafine (<0.1 microns) particles are most susceptible to sorption. Their negative effects on the upper and middle respiratory tract leading to inflammation and allergic reactions are known [15]. Children exposed to ultrafine particles at an early age develop chronic cough and wheezing [16]. Due to the sorption of exhaust gases, atmospheric microparticles contribute to a decrease in the sensitivity of respiratory tract cells and hyperplasia of goblet cells [17], which increases the occurrence of cancer processes. In addition to exhaust gases, polycyclic aromatic hydrocarbons are sorbed on the surface of microparticles, which exert oxidative stress. Accumulating in the body leads to problems with the cardiovascular and nervous systems [16]. Moreover, it is known that organic substances extracted from the surface initiate oxidative DNA damage, which leads to mutations [18]. Studies have been conducted that confirm the growth of diseases associated with exposure to atmospheric microparticles, such as bronchopulmonary pathologies [19], high blood pressure [20], increased blood clotting and the likelihood of thrombosis [21], oncology [22], asthma [23].

At the same time, the chemical [24], microbiological [25] composition of aerosol dust and the danger to people are investigated. The mineralogical composition of atmospheric microparticles has been studied by some scientists in the areas of dust storms [10,26,27]. In our opinion, there are very few such studies in semiarid regions.

The study of atmospheric microparticles makes it feasible to forecast the expectative properties of the soil cover, to elucidate the mechanisms initiating dust storms and other meteorological phenomena, to look into the wind erosion process and minimize the negative impact on living organisms. Systematized knowledge on the performance of atmospheric microfine particles, their buildup and translocation will help reduce their negative effect and solve a number of environmental challenges.

The aim of this research is to identify the characteristic diagnostic features of atmospheric microparticles that can be used to detect natural and man-made sources of their formation. The main tasks are to carry out a comprehensive morphological and mineralogical analysis of microparticles of natural and technogenic origin at various hierarchical levels and identify the alleged sources of dust fallout.

2. Materials and Methods

Field research was implemented in 2020 in the town of Istra, Moscow region. A sampling of dust was carried out on the roof of the State Historical and Art Museum "New Jerusalem", created using the green roof technology. The museum is located 300 m from the New Jerusalem Monastery (Figure 1). Previously, the authors performed studies of the soil cover of the Istra River valley, including the territory of the monastery itself and the park zone [28,29].

2.1. Sample Collection

Dust samples were collected by Gravimetric Settling of microparticles from the atmosphere into exposed Petri dishes (from August to October), similar to the method described earlier [25], at four sampling points, at a height of 16 m above ground level. In addition, road dust samples were taken at three sampling points: on the side of Buzharovskoe highway (D2); by a dirt road in a park area that adjoins the walls of the New Jerusalem Monastery (D1), and in the parking lot at the entrance to the park (D3) (Table S1).

At the first key site, 4 sample collection points were selected (R1–R4), and at three roadside sites—one point each (D1–D3), samples were taken seven times, a total of 49 samples were taken.

Figure 1. Sampling sites for atmospheric microparticles.

2.2. Calculation of Dust Load

The dust load was calculated using the formula: P = Pa/(ST), where Pa—weight of the deposited dust, kg; S—the projective area of the deposition (3.14 R^2) km^2; T—time interval (temporary interval) of the experiment, in days.

2.3. Granulometric Composition of the Samples

Size distribution of dust particles performed on a Microtrac Bluewave particle size analyzer (Microtrac, Montgomeryville, USA). The sample circulation rate in the system was 50% of the maximum (~33 mL/s) [30].

2.4. Statistical Analysis

Statistical calculations were made using the Statistica 8 soft.

2.5. Individual Particle Analysis

Microparticles were examined at various hierarchical levels using a binocular, a scanning electron microscope (hereinafter referred to as SEM) with microprobe analyzer with EDX system. Some of the samples were treated with hydrogen peroxide to remove films from the surface of mineral grains for subsequent study of the morphology of the grain surface using microscopy. The proportion of particles of various genesis was determined by counting the number of objects of mineral, biogenic and technogenic origin by the immersion method [31]. Average samples of 300 microparticles were formed, in which counting was carried out using a polarizing microscope MP-201. Particles up to 20 microns in size were quantified. Smaller fractions were evaluated qualitatively on the SEM. For each particle in our study, we examined 3–5 regions on the SEM EDX depending on the inhomogeneity of the particle.

2.6. SEM-EDX Analysis (Energy Dispersive X-ray Analysis)

Individual aerosol particles were analyzed manually by using SEM JEOL JSM-6380LA of the Faculty General Laboratory of Electron Microscopy, Faculty of Biology, Lomonosov Moscow State University. The SEM-EDX analysis was carried manually by using out with SEM (LEO 1450 VP, Carl Zeiss, Jena, Germany) equipped with an energy dispersive X-ray system INCA Energy 300 (OXFORD INSTRUMENTS ANALYTICAL), of Faculty of Geology, Lomonosov Moscow State University. A very thin film of gold and platinum (Au-Pt) was deposited on the surface of each sample using vacuum coating unit called JFC 1600 (Japan Electron Optics Laboratory (JEOL), Tokyo, Japan) which can prepare 4 samples at a time. The fine coating of gold and platinum makes the samples electrically conductive. The working conditions were set at an accelerating voltage of 20 kV, a beam current of 40–50 μA and a Si (Li) detector 10 mm away from the samples to be analyzed. The EDX analysis was carried out at each analysis point and the elements present were both qualitatively and quantitatively measured. The weight percentage of each element present in the spectrum was identified. On normalization to 100% for C and O, the weight percentage of different elements were also identified. Approximately 150 particles were analyzed on each sample to examine particle morphology, size (equivalent projected area diameter), and elemental composition. For each repetition, a sample was mounted on a copper stage using double-sided adhesive carbon tape. Then, the stages were gold coated to a thickness of 15 nm using a sputter coater for better conductivity and, therefore, reducing electron charge. The EDX spectrum was obtained by the irradiation of electron beams at the center of individual particles with accelerating volt age 20 kV and a counting time 60–100 s. 1500 particles were analyzed.

2.7. Heavy Metals in Road Dust

The determination of the gross forms of trace elements and heavy metals in microparticles of the samples was accomplished in the isolated fraction less than 0.1 mm [24] X-ray fluorescence on a Bruker S2Picofox device.

2.8. Natural Conditions of the Research Area

The climate is moderately continental with warm summers and moderately cold winters. The average annual air temperature is +3.3 °C, January −10.5 °C, July +17.1 °C [32]. Average annual precipitation is 537 mm. The prevailing winds are from the south-west, south and west directions. The vegetation cover of the study area belongs to the southern taiga zone with a predominance of coniferous–deciduous subtaiga forests [33].

Relief. In geomorphological terms, a floodplain and 2 floodplain terraces are identified on the territory. The first terrace above the floodplain stretches in a narrow strip, bordered by the monastery hill in the north and southwest, the surface of which is surrounded by slopes of various heights and steepness from all sides, except the east. The second terrace above the floodplain is flat, the maximum height being 162.5 m. The monastery is located on a hill-like rise, the height of which reaches 162.0 m [34].

Soil-forming rocks are mantle loams underlain by fluvioglacial and moraine deposits of the Moscow glaciation. Technogenic deposits are abundant on the territory of the monastery hill and in areas of fast-paced economic activity [34]. They are represented by clayey soils, sands with inclusions of construction waste and broken bricks. Modern alluvial deposits are prevalent in the river floodplain and are typified by silty gray sands and loams of medium density and size. Upper Quaternary deposits of the first above-floodplain terrace are constituted by light yellow sands of various sizes, as well as brown silty loams. The total thickness of the deposits of the first above-floodplain terrace is 6.9 m. Upper-Quaternary deposits of the second above-floodplain terrace are represented by brown and yellowish-brown sands of medium size, turning into coarse ones with interlayers and lenses of clay loams and inclusions of pebbles and gravel.

Soil cover. Owing to the long history of the transformation of the landscape portraying the territory of the Istra river valley adjacent to the monastery, the soil cover includes

both natural soils of the floodplain and anthropogenic ones located on the second terrace above the floodplain. The soil cover is dominated by alluvial soils of the floodplain—Gleyic Fluvisol (Aric, Siltic). Although in general they retained the morphological features characteristic of alluvial soils, the construction of the Istra reservoir led to a change in their properties. The first above-floodplain terrace is formed by Fluvisol (Loamic, Calcaric), experiencing anthropogenic pressure due to the recreational use of the territory. We described Urbic Technosol (Calcic, Humic, Loamic) on the technogenic deposits of the second above-floodplain terrace, and Urbic Technosol (Arenic, Eutric, Transportic) [28,29].

Ecological situation. According to the degree of transformation of the natural environment, the research area is classified as natural—technogenic. There are no large factories or plants in the vicinity; the region itself has a low share of industrial land (4–6%). The main air pollutants in the Istra district are carbon monoxide, nitrogen dioxide and sulfur, combustion processes, industrial influences and vehicle exhaust emissions being major contributors to form these substances. The territories sited along the highways (Moscow-Volokolamsk, Moscow-Riga, three highways of the Central Ring Road), as well as territories situated in close proximity to large industrial enterprises (Novo-Jerusalem plant, Zheleznyakovskaya Petelinskaya poultry farm) are experiencing the greatest stress [35]. We regard these factories and highways as presumptive provenance of solid atmospheric deposition in the study area. The dominant sources of soil pollution appear to be household waste generated by the population, sewage, and chemicals used in agriculture. The analyses for the presence of heavy metals in the soil showed that the city is in a relatively favorable ecological situation; still, it is worth paying attention to the enterprise-neighboring areas, which were assigned to the moderately dangerous category [36].

3. Results and Discussion

3.1. Investigation of Atmospheric Microparticles Sampled on the Roof

During the collection of microparticles by gravimetric precipitation on the roof of museum complex the dust load was 95.03 ± 56.32 kg/sq·km·day (n = 28). According to studies conducted in Russia, the dust load for the park area of Moscow is 64–175 kg/sq·km·day [25].

As a result of morphological analysis of the selected samples under a binocular microscope, atmospheric microparticles of three groups were isolated: biogenic, mineral, and technogenic. It should be noted that the number of particles of technogenic origin, including fragments of plastic, glass and brick chips, is scarce and is exemplified by single particles in dust samples taken from the roof.

Microparticles of biological origin are available in large numbers by leaf fragments, seeds, pollen, insect bites (Figure 2a,b; sample R1). The samples taken on the roof at the point located on the side of Nikitino village were distinguished by a significant diversity of the organic component. There are abundant dark plant remains that have preserved cellular structure, hyphae of fungi and micromycetes, specks of the chitinous cover of insects, and diatoms (Figure 2a–f; sample R1). The presence of the latter characterizes the role of hydromorphic landscapes of the river valley. Particles of biogenic origin are small (from 5–10 microns), whereas large objects (from 600 microns) are less common. Smaller mineral particles are adsorbed on the surface of large plant residues. Accumulations of objects of biological origin can also be observed on the surface of large mineral grains (Figure 3a–d; sample R2).

Most of the studied samples are mineral particles, among which quartz grains of varying roundness prevail (Figure 4; sample R1). Less common are feldspars, biotite, and calcite (Figure 5; sample R3). There prevail rounded particles (Figure 6a,b; sample R1) up to 400 microns in size, angular grains characterized by a glossy surface, the size of which varies from 100 to 500 microns. Most of the mineral grains are covered with clay films (Figure 6c,e; sample R2), often with a clearly expressed plaque of fine dusty microparticles on the mineral grains (Figure 6d; sample R1).

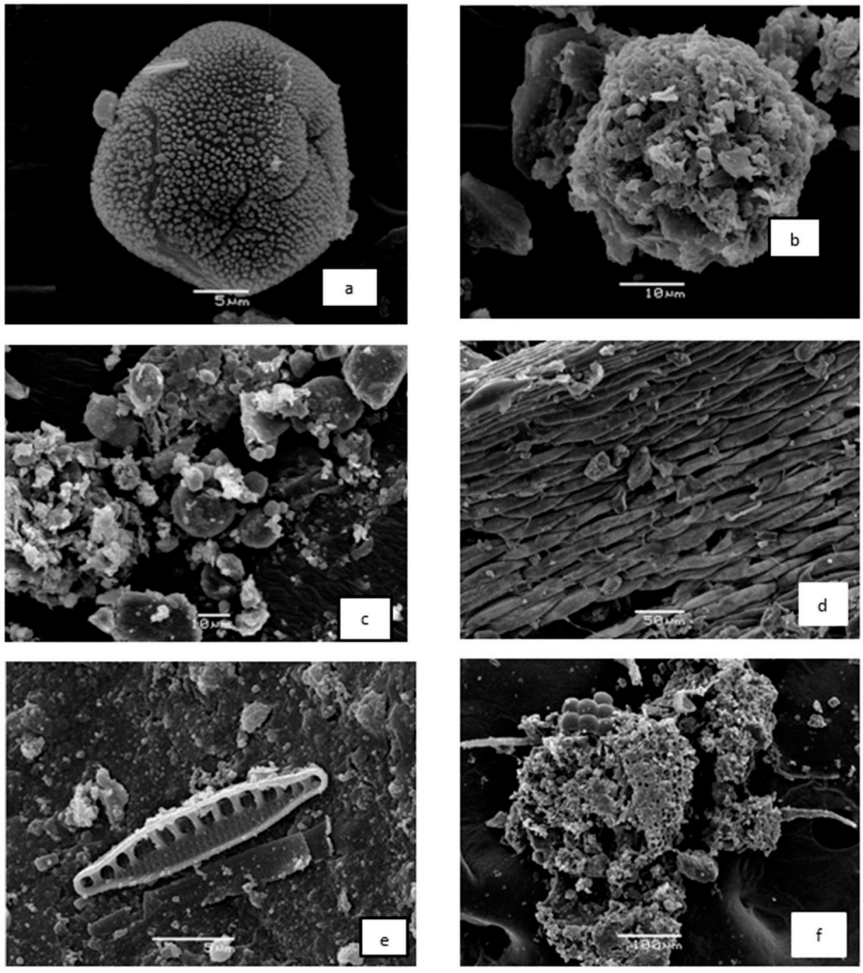

Figure 2. Atmospheric microparticles of biological origin: (**a**)—pollen grains; (**b**,**c**)—shell amoebas; (**d**)—insect tissue remains; (**e**)—diatoms; (**f**)—perforated plant tissue. SAM JSM-6380 LA. The scale is 5 μm (**a**,**e**), 10 μm (**b**,**c**), 50 μm (**d**) and 100 μm (**f**).

In addition to individual mineral grains, aggregates are found (Figure 7; sample D2). The grains of quartz and feldspars, which are part of the aggregates, are irregular in shape, strongly corroded, their size varying from 5 to 10 microns.

The aluminosilicate composition of microparticles and the presence of clay films on the surface of mineral grains give grounds to assume that the particles are of rock-soil origin. The mineralogical composition of microparticles reflects the ecological and geographical conditions of their emergence, namely the Central Russian mineralogical province [37]. The morphological and mineralogical analysis made it possible to determine the component composition of the samples and the approximate proportions of various groups of microparticles. Dust samples on the roof contain less than 1% technogenic particles and approximately 40% biogenic particles (Figure 8). The rest of the mass is made up of mineral grains. In road dust samples, the proportion of technogenic particles increases to 15%, while biological objects make up 5%. Most of the samples are made up of mineral particles. The proportion of particles of different genesis in the sampling of the dust are presented in Figure 8.

3.2. Features of the Surface Morphology of Mineral Grains

The micromorphological analysis of the grain surface is based on the idea that the grains inherited from the minerals of the bedrock acquire certain morphological features that are characteristic of those environments where their transfer and accumulation occur [38,39]. The surface morphology of mineral particles can serve as an indicator of

environmental pollution by various toxic agents [40,41]. At present, significant data have been accumulated on the genesis of the main types of morphostructures of mineral grains [38,39,41–43].

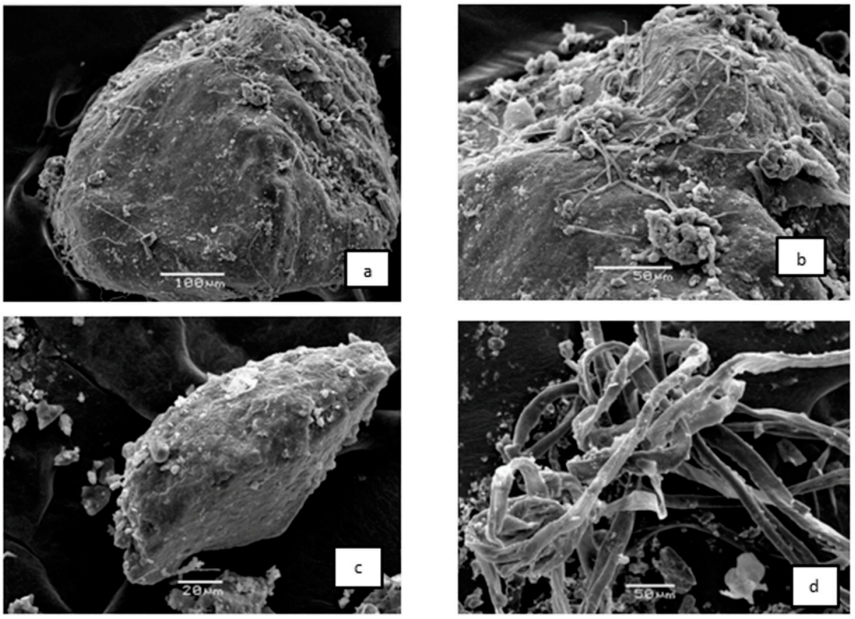

Figure 3. Atmospheric microparticles of biological origin on the surface of mineral grains: (**a**,**b**)—hyphae-micromycetes; (**c**)—Microorganisms on the surface of mineral particles; (**d**)—Hyphae of fungi. SAM JSM-6380 LA. The scale is 100 μm (**a**), 50 μm (**b**,**d**), 20 μm (**c**).

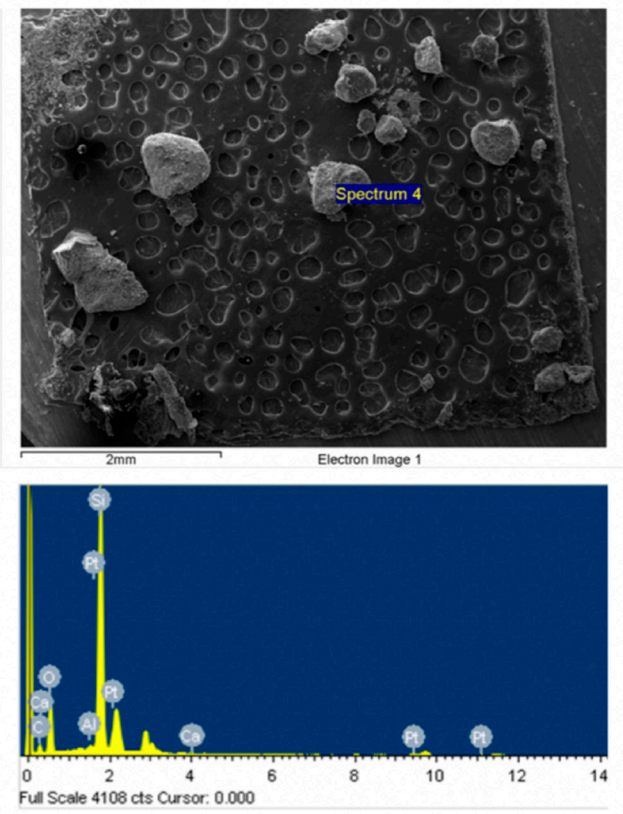

Spectrum processing :
Peak possibly omitted : 3.021 keV

Processing option : Oxygen by stoichiometry (Normalised)
Number of iterations = 6

Standard :
C CaCO3 1-июн-1999 12:00 AM
Al Al2O3 1-июн-1999 12:00 AM
Si SiO2 1-июн-1999 12:00 AM
Ca Wollastonite 1-июн-1999 12:00 AM

Element	Weight%	Atomic%	Compd%	Formula
C K	16.49	22.54	60.44	CO2
Al K	0.24	0.15	0.46	Al2O3
Si K	18.18	10.63	38.90	SiO2
Ca K	0.15	0.06	0.20	CaO
O	64.93	66.62		
Totals	100.00			

Figure 4. Energy dispersive spectrum of quartz grain. SAM LEO 1450 VP, Carl Zeiss.

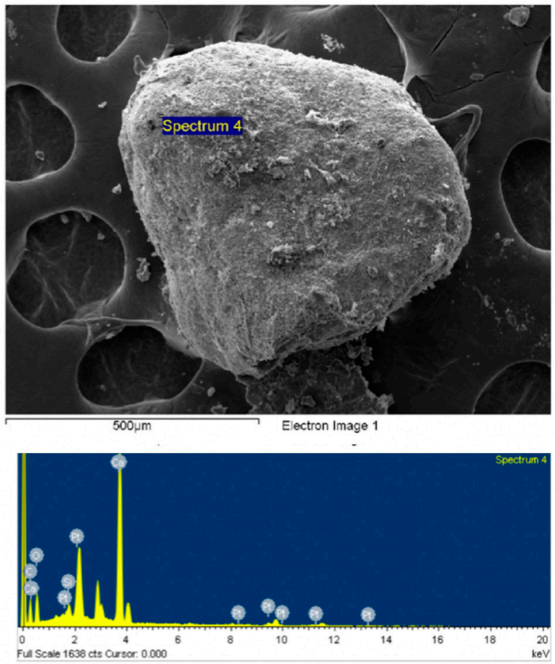

Spectrum processing :
Peaks possibly omitted : 1.265, 3.016 keV

Processing option : Oxygen by stoichiometry (Normalised)
Number of iterations = 3

Standard :
C CaCO3 1-июн-1999 12:00 AM
Si SiO2 1-июн-1999 12:00 AM
Ca Wollastonite 1-июн-1999 12:00 AM

Element	Weight%	Atomic%	Compd%	Formula
C K	19.86	27.77	72.76	CO2
Si K	0.72	0.43	1.54	SiO2
Ca K	18.37	7.70	25.70	CaO
O	61.05	64.10		
Totals	100.00			

Figure 5. Surface morphology and energy dispersive spectrum of calcite. SEM LEO 1450 VP, Carl Zeiss.

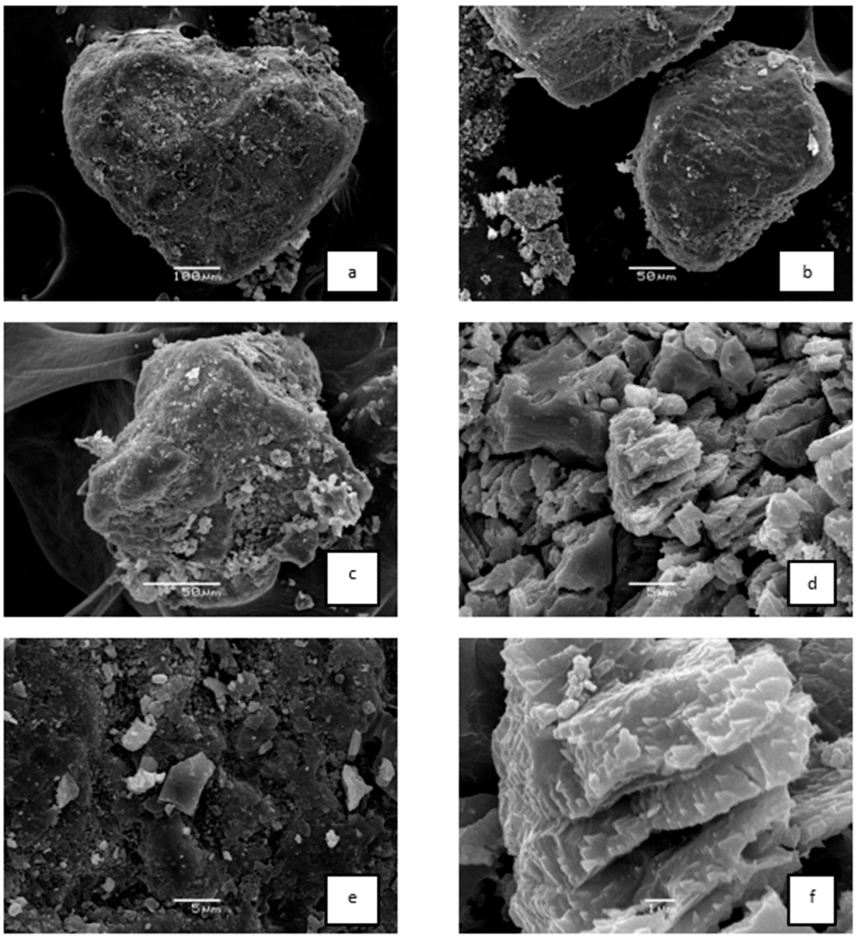

Figure 6. Mineral grain morphology. (**a**,**b**)—quartz grains of various shapes; (**c**,**e**)—quartz grain covered with film; (**d**,**f**)—Weathered feldspar grains covering the grain of quartz. SAM JSM-6380 LA. The scale is 100 µm (**a**), 50 µm (**b**,**c**), 5 µm (**d**,**e**), 1 µm (**f**).

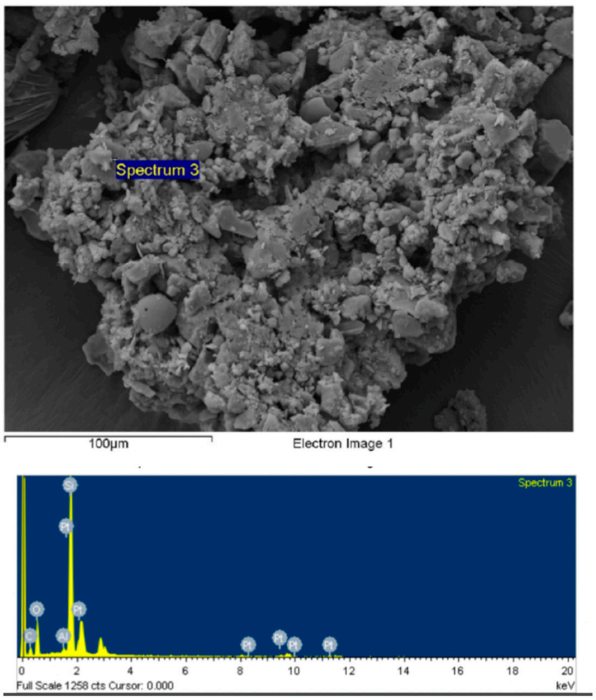

Spectrum processing :
Peak possibly omitted : 3.020 keV

Processing option : Oxygen by stoichiometry (Normalised)
Number of iterations = 7

Standard :
C CaCO3 1-июн-1999 12:00 AM
Al Al2O3 1-июн-1999 12:00 AM
Si SiO2 1-июн-1999 12:00 AM

Element	Weight%	Atomic%	Compd%	Formula
C K	18.00	24.19	65.94	CO2
Al K	0.36	0.22	0.68	Al2O3
Si K	15.60	8.97	33.38	SiO2
O	66.04	66.63		
Totals	100.00			

Figure 7. Morphological structure of a loose aggregate including mineral microparticles and EMF of one of the grains. SAM LEO 1450 VP, Carl Zeiss.

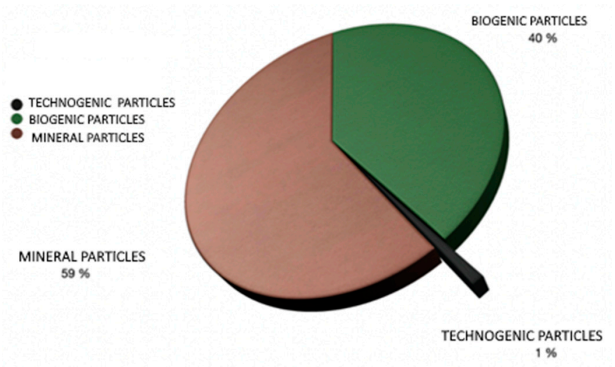

(**a**)

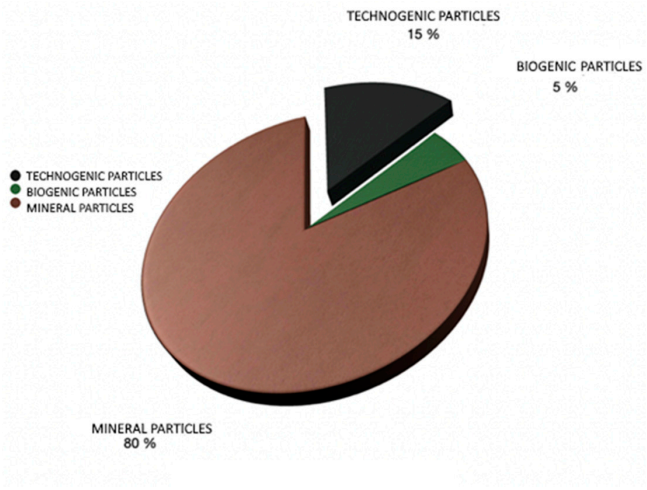

(**b**)

Figure 8. The proportion of particles of different genesis in the sample from the roof (**a**) and road dust (**b**).

Drawing on the study of the surface of quartz grains under a binocular microscope and an electron-scanning microscope, several groups of primary morphostructures were identified. The first group includes well-rounded grains with a matte surface ranging in size from 100 to 250 microns. Micro-grooves and grooves on the surface are up to 10 μm; on some particles, a shell-like fracture is noted. The second group includes poorly rounded grains of irregular shape with an uneven surface, up to 400 microns in size, with clay films noted on them, which indicates the influence of soil-forming processes; stepwise and conchoidal fractures are characteristic. The sizes of the chips vary from 50 to 150 μm, micro-grooves up to 10 μm (Figure 9a). Among the studied samples, particles of the first and second groups predominate. Judging by the size of mineral grains, the absence of pointed chips and a matte surface, one can assume that they belong to the aeolian environment of short-distance transport, their mineralogical composition being similar to that of soils previously delved by the authors in the study area.

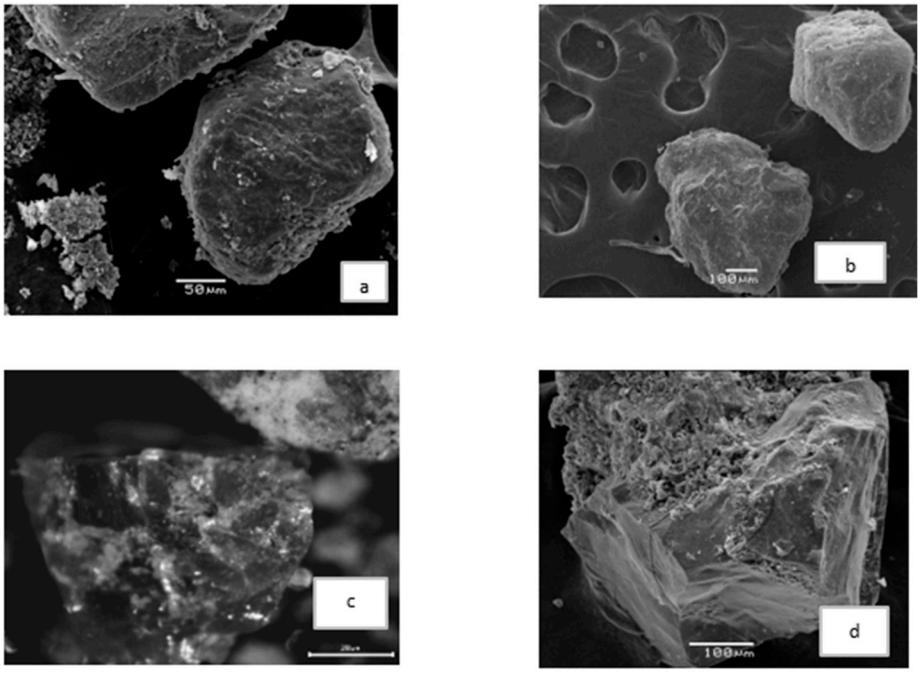

Figure 9. Surface morphology of quartz grains: (**a**)—microdeposits; (**b**,**d**)—stepped cleavage; (**c**)—glossy surface. Binocular (**c**). SAM JSM-6380 LA. (**a**,**b**,**d**). The scale is 50 μm (**a**), 100 μm (**b**,**d**), and 20 μm (**c**).

By the size of mineral grains, the third group includes large (from 500 to 700 μm) acute-angled mineral grains with pronounced edges, glossy shiny surface (Figure 9c) and stepped chips of large and medium sizes (from 300 μm) (Figure 9b,d). There are isometric grains with sharp edges and even chips of various sizes. The size, shape and nature of the chips and shiny surfaces suggest that the predominant formation medium is the glacial mineral grains of the third group.

The results of a submicromorphological study of the surface of mineral quartz grains (Figures 6 and 9) of the studied samples indicate the predominance of the aeolian medium for transporting material over short distances, which is expressed in the rounded shape of atmospheric microparticles and their matte surface with small grooves. The formation of textures of aeolian genesis is influenced not only by the mechanical factor, but also by chemical weathering, which affects the formation of the matte surface of the mineral grain and matte pits. The soil-rock origin of the particles is evidenced by the presence of clay films on their surface.

3.3. Road Dust Research

Particle sizes. The investigated road dust has a light granulometric composition with a predominance of fractions of fine sand and coarse dust (Figure 10).

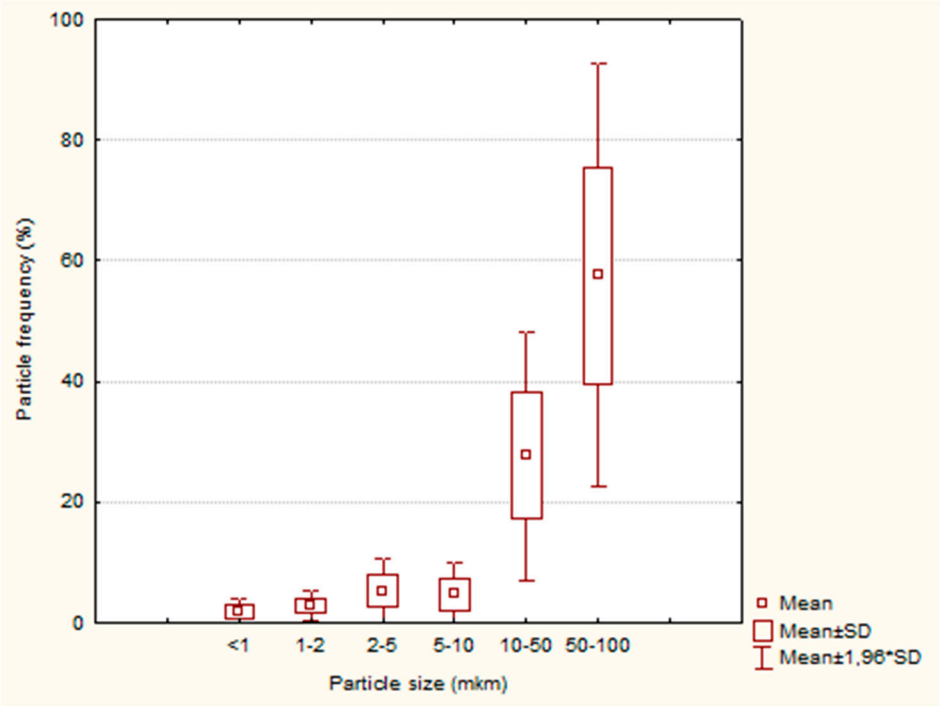

Figure 10. Box plot of particle size fraction in road dust in percent by volume.

Road dust samples have increased levels of technogenic microparticles, including asphalt chips, metal particles, glass shards and plastic fragments. Many researchers have noted the presence of microplastics among urban air pollutants [44,45]. The mineral constituent is presented in the form of poorly rounded grains, quartz predominates in the material, and grains of calcite (Figure 11a; sample D3) and biotite (Figure 11b; sample D3) are also found. Quartz grains often have black streaks. The proportion of particles of biological origin represented by plant residues is much smaller.

3.4. Content of Heavy Metals and Trace Elements in Road Dust Samples

The statistical indicators of the total content of heavy metals in road dust and in the upper horizon of background soil are presented in Table 1. Currently, Russia has not developed standards of limit or guidelines of heavy metal in deposited dust. The average content of all investigated heavy metals in the road dust upper than in background soils, except manganese. The excess of heavy metals content in dust compared to soils was noted by many researchers of urban dust in Russia [24] and other countries [46]. It is reasonable to compare the content of heavy metals in dust with the content of heavy metals in spatially related soils, since street dust is partly of soil origin. The increased content of heavy metals in dust compared to soils indicates a high enrichment of dust with modern atmospheric fallout.

Table 1. Statistical Indicators of Metal Content in road dust samples and Background Soils (mg kg^{-1}).

Heavy Metal	Cr	Mn	Fe	Co	Ni	Cu	Zn	Sr	Cd	Pb
					road dust samples					
Mean	27.15	357.84	14.086.56	5.34	12.16	23.09	73.15	57.87	0.19	11.42
Median	23.68	334.5	13.670	5.22	12.73	18.3	68.44	57.1	0.2	11.75
Standard deviation	7.48	56.15	1943.84	0.25	0.93	13.73	26.94	11.45	0.05	2.63

Table 1. *Cont.*

Heavy Metal	Cr	Mn	Fe	Co	Ni	Cu	Zn	Sr	Cd	Pb
Min	19.54	296.9	11.670	5.09	10.66	10.24	42.57	44.14	0.12	7.4
Max	37.28	437.9	17.210	5.75	12.91	43.34	107.9	72.27	0.25	14.62
Coefficients variation, %	27.54	15.69	13.80	4.60	7.62	59.47	36.83	19.79	25.24	23.02
Background Soil										
Mean	21.93	495.75	13.655.67	4.8	11.35	8.82	37.52	37.45	0.16	8.7
Median	22.19	494.18	13.615	4.88	11.2	9.14	37.04	37.15	0.17	9.05
Standard deviation	0.85	10.63	157.98	0.19	0.34	0.73	1.26	0.52	0.01	1.24
Min	20.98	486	13.522	4.58	11.1	7.98	36.58	37.15	0.15	7.32
Max	22.63	507.08	13.830	4.94	11.74	9.33	38.95	38.05	0.17	9.72
Coefficients variation, %	3.90	2.14	1.16	4.03	3.03	8.30	3.35	1.39	7.71	14.26

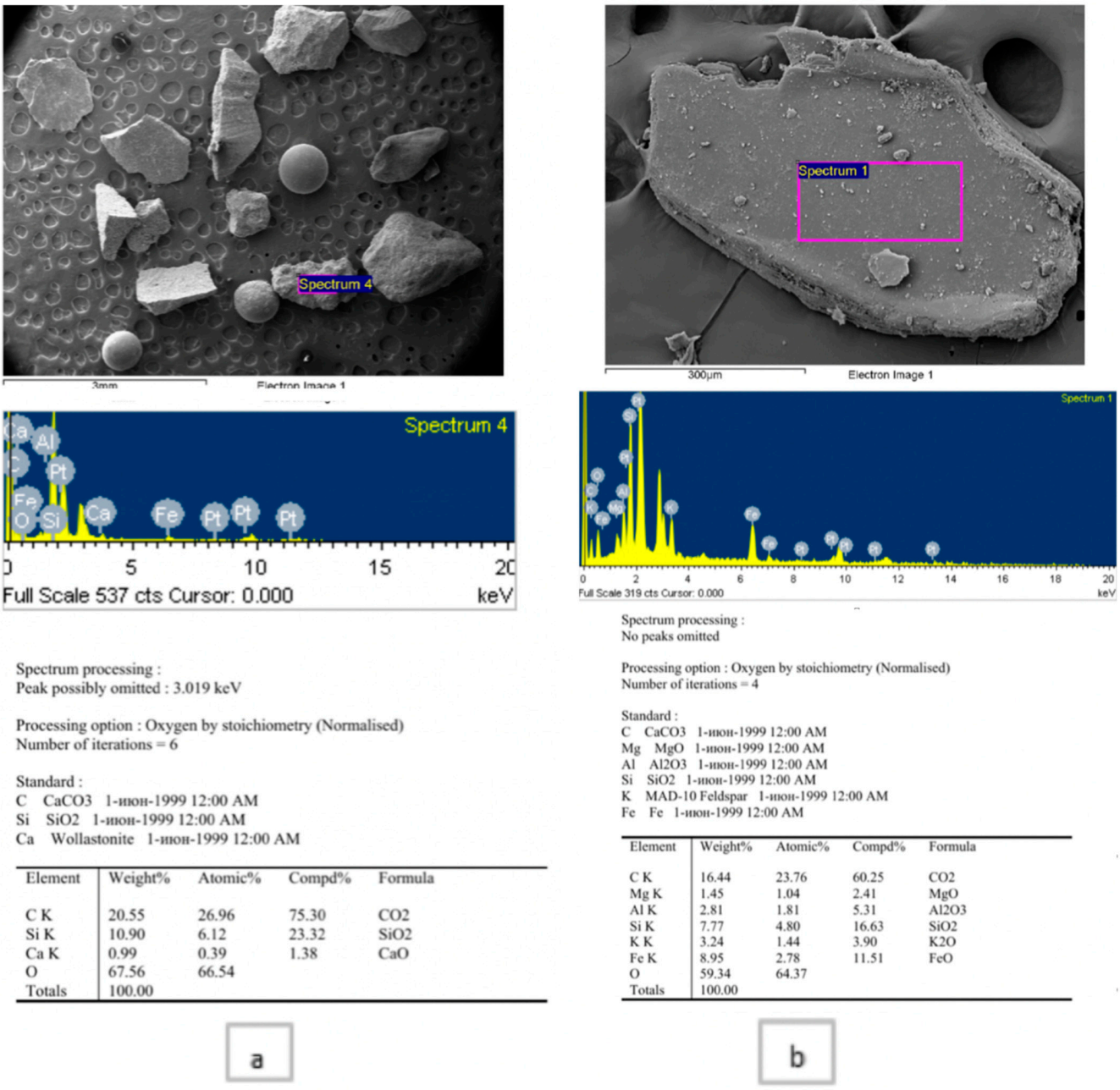

Figure 11. Morphology and energy dispersive spectra of road dust microparticles: (**a**)—calcite grain; (**b**)—biotite.

The Geoaccumulation Index (Igeo) was calculated to identify the degree of contamination of road dust with heavy metals. The index was proposed by Muller as a geochemical criterion for pollution detection [47]. It was widely used to assess the level of contamination of soils and road dusts of certain heavy metals.

Geoaccumulation Index was calculated using the following formula:

Igeo = log2(Ci/1.5BG), where Ci—content of heavy metals in the upper horizon, BG—background content in soil.

Igeo ranges seven sediments condition classes (Table 2) (given by [48]).

Table 2. Classes of Igeo in Relation to Pollution Levels and Enrichment, respectively.

Class	I_{geo}	
	Value	Designation of Street Dust Quality
0	Igeo $\leq$ 0	Not polluted
1	0 < Igeo $\leq$ 1	No to moderate pollution
2	1 < Igeo $\leq$ 2	Moderately polluted
3	2 < Igeo $\leq$ 3	Moderately to heavily polluted
4	3 < Igeo $\leq$ 4	Heavily polluted
5	4 < Igeo $\leq$ 5	Heavily to extremely polluted
6	Igeo > 5	Extremely polluted

Box plot for the Geoaccumulation Index of heavy metals in road dust is shown in Figure 12. The most investigated heavy metals, such as Cr, Mn, Fe, Co, Ni, Cd, Pb, have a value of Geaccumulation Index of road dust average below zero in Istra city, which suggested the absence of accumulation of those heavy metals in the road dust in this small town near Moscow. The level of pollution of road dust for strontium, zinc and copper is mild to moderate. Geoaccumulation Index for average in this case is located in ascending order from stroncium to copper in the following order Sr < Zn < Cu (0.02 < 0.29 < 0.58). The appearance of Box plot is indicative of the distribution of Igeo being close to normal, which also confirms the absence of significant technogenic pollution of the investigated road dust.

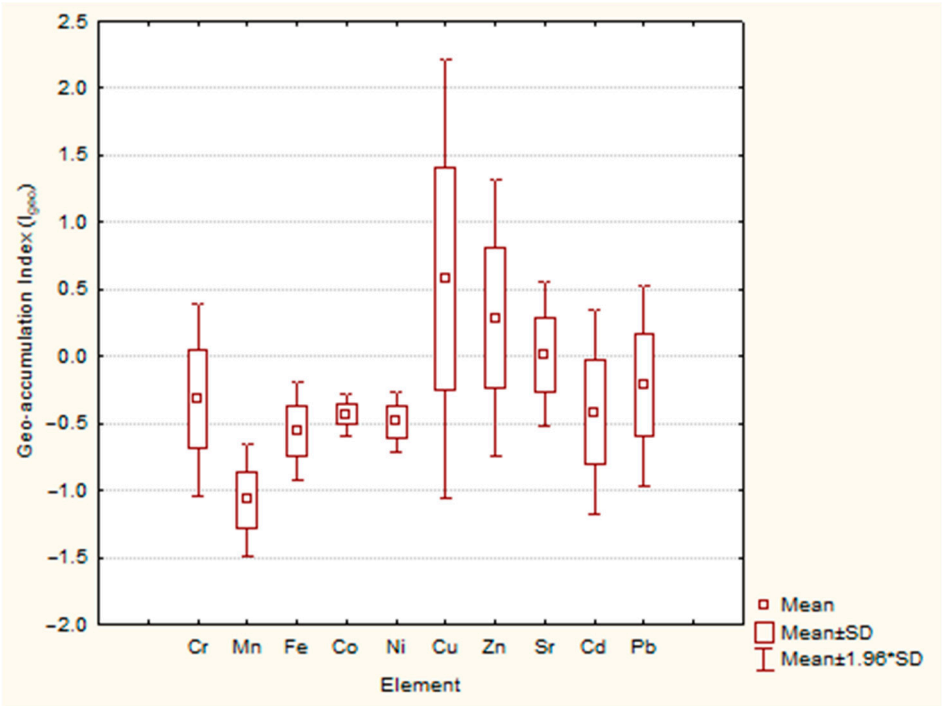

Figure 12. Box plot of Geoaccumulation Index of heavy metals in the road dust.

3.5. Enrichment Factor

Enrichment Factor (EF) is a measure of possible influence of anthropogenic activity on concentration of heavy metals in soil [49]. The content of heavy metals characterized by low variability of occurrence both in analyzed samples and in background soils is used as a reference. As control elements, usually Fe, Al, Ca, Ti, Sc or Mn, are used. We used Fe as the reference element [50]. EF was calculated using the following formula:

$$EF_{Fe} = (Ci/C_{Fe})\ \text{sample}/(Ci/C_{Fe})\ \text{background}.$$

There are five levels of metals accumulation. These are minimum (EF < 2), moderate (2–5), significant (5–20), very high (20–40), extremely high (>40). If EF value ranges from 0.5 to 1.5, the content of this heavy metal in soil is considered to be caused by natural processes. However, if EF value exceeds 1.5, then there is a possibility that the pollution by heavy metals has occurred as a result of anthropogenic activities [51].

The content of most heavy metals in the road dust of the Istra city, such as Cr, Mn, Fe, Co, Ni, Cd, Pb is caused by natural processes, this judged by the average values of EF, which fit into the range of 0.5–1.5 for this metal (Figure 13). The average values of EF for Cu, Zn and Sr exceed 1.5, which indicates anthropogenic enrichment. Yet, the enrichment of zinc and strontium is minimal, and copper has an average level of anthropogenic accumulation in road dust.

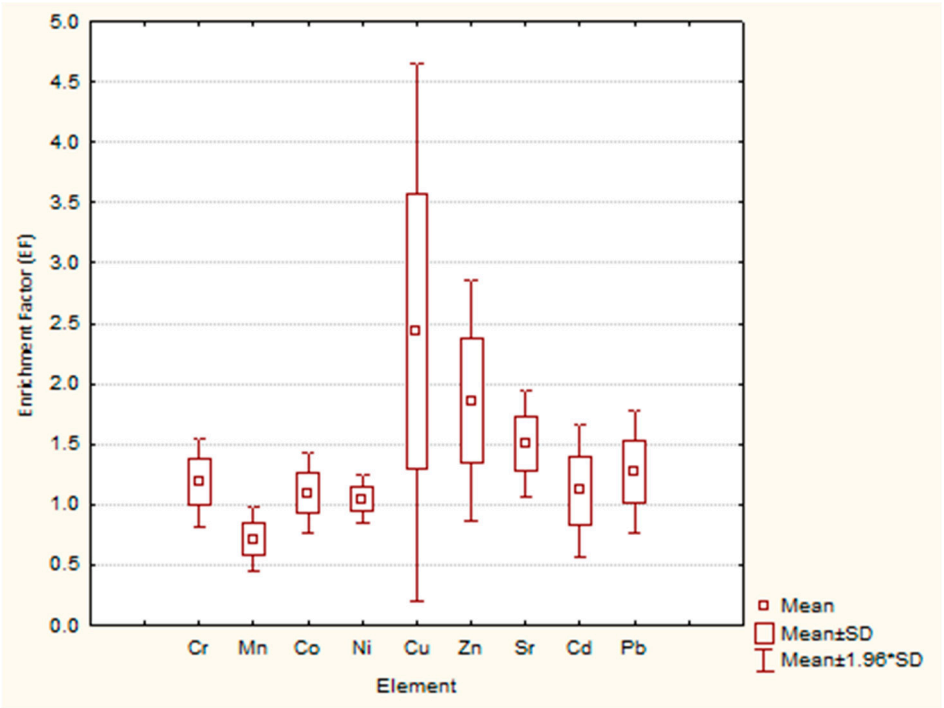

Figure 13. Box plot of Enrichment Factor (EF) of heavy metals in road dust.

The use of the Enrichment Factor to assess the degree of technogenic impact on the investigated area enables a more accurate assessment as compared to Igeo, which is less informative. The road dust compared to the other natural objects, for example, soil, makes it possible identify even a small technogenic impacts more accurately, since the proportion of technogenic compounds per mass unit of dust is more than per mass unit of soil. The investigated area is characterized by low technogenic impact on the natural environment. Based on the analysis of road dust, it was found that there is a slight increase in the content of copper, zinc, and strontium.

The high content of Al and Si in the dust composition argues the aluminosilicate origin of the particles. Thus, the results of determining the material composition of dust indicate

that road transport is one of the main sources of technogenic microparticles that contribute to the pollution of natural objects. In general, the ecological situation in the Istra region is quite favorable.

In the city of Istra in 2020 due to the pandemic, the work of some enterprises (a cement plant) was stopped and most of the production facilities reduced the volume of work. The main polluter in the city was public transport. Therefore, it can be recommended to strengthen the control of compliance of road transport with environmental regulations and to develop a public transport network, which will reduce car traffic.

4. Conclusions

Complex studies of atmosphere microparticles, collected by the sedimentation way, and the samples of road dust in urban condition have been carried out.

The complex studies have revealed the multicomponent composition of atmospheric microparticles. Most of the samples are represented by mineral grains; they also include particles of organic origin of various genesis and technogenic particles (Figure 8).

In the content of road dust predominant by fractions of fine sand and coarse dust.

The morphological and mineralogical features of dust particles reflect the mineralogical and geochemical features of the region of their origin. These data can be used to clarify the regional affiliation of dust samples. Mineralogical and geochemical provinces are distinguished by the origin and composition of the mineral components of soils and sediments [37]. Micromorphological features of the particle surface reflect the processes and changes that took place during the formation and transfer of microparticles. Grains of quartz and feldspars, characteristic of the Central Russian mineralogical province [37], predominate, indicating the rock-soil origin of microparticles. This is also confirmed by the presence of clay films on the surface of mineral grains and the presence of aggregated material.

The results of the submicromorphological study of the surface of mineral quartz grains indicate the predominance of the aeolian medium for transporting material over short distances, which is expressed in the rounded shape of atmospheric microparticles, their matte surface with small grooves.

The abundance of organic component in the dust samples is associated with the influence of the forest and vast areas occupied by meadow vegetation, typical of floodplain landscapes.

The abundance of biological components in the composition of dust and an insignificant participation of technogenic microparticles characterize a favorable ecological situation in the research area.

The main source of pollution is road dust, however, no significant excess of the MPC for pollutants has been identified.

The average content of all investigated heavy metals in the road dust is higher than in background soil (except manganese). The level of pollution of road dust by strontium, zinc and copper ranges from minimal to moderate. The enrichment in zinc and strontium is minimal, and copper has an average level of anthropogenic accumulation in the road dust. The assessment of the technogenic impact on the territory with the calculation of the Enrichment Factor revealed a low level of the technogenic impact on the natural environment. When assessing the ecological state of the natural environment, the landscape should be noted, namely the ecological role of park massifs and floodplain meadows, which take up a significant share of the investigated area.

Atmospheric particles harm human health due to the sorption of pollutants on their surface. The main parameters of the particles causing biological influence are the surface area and character, as well as the diameter of the particles [18]. The study of the mineralogical composition and micromorphology of suspended solids up to 20 microns in size allowed us to conclude that there is no global transfer of dust aerosol from other regions. Films and fixed particles of a thinner size were found on the surface of these particles.

Supplementary Materials: The following supporting information can be downloaded at: https://www.mdpi.com/article/10.3390/atmos14020403/s1, Table S1: The details of sample collection in Istra.

Author Contributions: Conceptualization: V.M.K. and O.A.S.; methodology, V.M.K. and O.A.S.; data curation, V.M.K. and O.A.S.; field trip, V.M.K., O.A.S., V.Y.V. and A.S.S.; investigation, V.M.K., O.A.S., D.V.L. and A.S.S.; data curation, V.M.K., O.A.S., V.Y.V. and A.S.S.; writing—original draft preparation, V.M.K.; writing—review and editing, V.M.K. and O.A.S.; visualization, V.M.K., O.A.S., V.Y.V. and A.S.S. All authors have read and agreed to the published version of the manuscript.

Funding: The study was carried out with the financial support of the Russian Foundation for Basic Research (RFBR) within the framework of scientific project No. 19-05-50093.

Institutional Review Board Statement: Not applicable.

Informed Consent Statement: Not applicable.

Data Availability Statement: The data from our previous studies of natural conditions and soil cover presented of the study are openly available at DOI: 10.1134/S1064229318090132 reference number [28] and at DOI: 10.1007/978-3-319-89602-1_6 reference number [29]. The full text of articles could be provided if necessary.

Acknowledgments: The authors would like to express their sincere gratitude to Sergey Shoba, who supervised the research project and supported the authors at all stages of their work.

Conflicts of Interest: The authors declare no conflict of interest.

References

1. Abdullaev, S.F. *Comprehensive Studies of Dust and Gas Impurities in Arid Zones and Their Impact on the Regional Climatic Regime of the Southeastern Part of Central Asia: D. Sc.: 25.00.30*; Russian State Hydrometeorological University: St. Petersburg, Russia, 2014.
2. Katola, V.M. Dust: Sources of formation, general characteristics, dust diseases (short review). *Bull. Physiol. Pathol. Respir.* **2018**, *67*, 111–116. [CrossRef]
3. Shao, L.Y.; Liu, P.J.; Jones, T.; Yang, S.S.; Wang, W.H.; Zhang, D.Z.; Li, Y.W.; Yang, C.-X.; Xing, J.P.; Hou, C.; et al. A review of atmospheric individual particle analyses: Methodologies and applications in environmental research. *Gondwana Res.* **2022**, *110*, 347–369. [CrossRef]
4. Li, J.; Shao, L.Y.; Chang, L.L.; Xing, J.P.; Wang, W.H.; Li, W.J.; Zhang, D.Z. Physicochemical Characteristics and Possible Sources of Individual Mineral Particles in a Dust Storm Episode in Beijing, China. *Atmosphere* **2018**, *9*, 269. [CrossRef]
5. Kellogg, C.A.; Griffin, D.W. Aerobiology and the global transport of desert dust. *Trends Ecol. Evol.* **2006**, *21*, 638–644. [CrossRef] [PubMed]
6. Wang, W.H.; Shao, L.Y.; Zhang, D.Z.; Li, Y.W.; Li, W.J.; Liu, P.J.; Xing, J.P. Mineralogical similarities and differences of dust storm particles at Beijing from deserts in the north and northwest. *Sci. Total Environ.* **2022**, *803*, 149980. [CrossRef]
7. Charlesworth, S.; Everett, M. A comparative study of heavy metal concentration and distribution in deposited street dusts in a large and a small urban area: Birmingham and Coventry, West Midlands, UK. *Environ. Int.* **2003**, *29*, 563–573. [CrossRef] [PubMed]
8. Moreno, T.; Merolla, L.; Gibbons, W.; Greenwell, L.; Jones, T.; Richards, R. Variations in the source, metal content and bioreactivity of technogenic aerosols: A case study from Port Talbot, Wales, UK. *Sci. Total Environ.* **2004**, *333*, 59–73. [CrossRef]
9. Suryawanshi, P.V.; Rajaram, B.S.; Bhanarkar, A.D.; Chalapati Rao, C.V. Determining heavy metal contamination of road dust in Delhi, India. *Atmósfera* **2016**, *29*, 221–234. [CrossRef]
10. Garofalide, S.; Postolachi, C.; Cocean, A.; Cocean, G.; Motrescu, I.; Cocean, I.; Munteanu, B.S.; Prelipceanu, M.; Gurlui, S.; Leontie, L. Saharan Dust Storm Aerosol Characterization of the Event (9 to 13 May 2020) over European AERONET Sites. *Atmosphere* **2022**, *13*, 493. [CrossRef]
11. Kasimov, N.S. Enrichment of road dust particles and adjacent environments with metals and metalloids in eastern Moscow. *Urban Clim.* **2020**, *32*, 100638. [CrossRef]
12. Hristova, E.S.; Manousakas, M.I. Special Issue: Air Pollution at the Urban and Regional Level: Sources, Sinks, and Transportation. *Atmosphere* **2023**, *14*, 132. [CrossRef]
13. Shao, L.Y.; Li, J.; Zhang, M.Y.; Wang, X.M.; Li, Y.W.; Jones, T.; Feng, X.L.; Silva, L.F.O.; Li, W.J. Morphology, composition and mixing state of individual airborne particles: Effects of the 2017 Action Plan in Beijing, China. *J. Clean. Prod.* **2021**, *329*, 129748. [CrossRef]
14. Yesilkanat, C.M.; Kobya, Y. Spatial characteristics of ecological and health risks of toxic heavy metal pollution from road dust in the Black Sea coast of Turkey. *Geoderma Reg.* **2021**, *25*, e00388. [CrossRef]
15. Veremchuk, L.; Mineeva, E. Impact of atmospheric microparticles and heavy metals on external respiration function of urbanized territory population. *Russ. Open Med. J.* **2017**, *6*, 402. [CrossRef]

16. Maier, K.L.; Alessandrini, F.; Beck-Speier, I.; Hofer, T.P.J.; Diabaté, S.; Bitterle, E.; Stöger, T.; Jakob, T.; Behrendt, H.; Horsch, M.; et al. Health Effects of Ambient Particulate Matter—Biological Mechanisms and Inflammatory Responses to In Vitro and In Vivo Particle Exposures. *Inhal. Toxicol.* **2008**, *20*, 319–337. [CrossRef] [PubMed]
17. Ji, H.; Khurana Hershey, G. Genetic and epigenetic influence on the response to environmental particulate matter. *J. Allergy Clin. Immunol.* **2012**, *129*, 33–41. [CrossRef]
18. Valavanidis, A.; Fiotakis, K.; Vlachogianni, T. Airborne Particulate Matter and Human Health: Toxicological Assessment and Importance of Size and Composition of Particles for Oxidative Damage and Carcinogenic Mechanisms. *J. Environ. Sci. Health* **2008**, *26*, 339–362. [CrossRef]
19. Veremchuk, L.V.; Vitkina, T.I.; Barskova, L.S.; Gvozdenko, T.A.; Mineeva, E.E. Estimation of the Size Distribution of Suspended Particulate Matters in the Urban Atmospheric Surface Layer and Its Influence on Bronchopulmonary Pathology. *Atmosphere* **2021**, *12*, 1010. [CrossRef]
20. Zanobetti, A.; Luttmann-Gibson, H.; Horton, E.S.; Cohen, A.; Coull, B.A.; Hoffmann, B.; Schwartz, J.D.; Mittleman, M.; Li, Y.; Stone, P.H.; et al. Brachial artery responses to ambient pollution, temperature, and humidity in people with type 2 diabetes: A repeated-measures study. *Environ. Health Perspect.* **2014**, *122*, 242–248. [CrossRef]
21. Bind, M.A.; Baccarelli, A.; Zanobetti, A.; Tarantini, L.; Suh, H.; Vokonas, P.; Schwartz, J. Air pollution and markers of coagulation, inflammation, and endothelial function: Associations and epigene-environment interactions in an elderly cohort. *Epidemiology* **2012**, *23*, 332–340. [CrossRef]
22. Nafstad, P. Lung cancer and air pollution: A 27 year follow up of 16 209 Norwegian men. *Thorax* **2003**, *58*, 1071–1076. [CrossRef] [PubMed]
23. Acosta, J.A.; Faz, Á.; Kalbitz, K.; Jansen, B.; Martínez-Martínez, S. Heavy metal concentrations in particle size fractions from street dust of Murcia (Spain) as the basis for risk assessment. *J. Environ. Monit.* **2011**, *13*, 3087–3096. [CrossRef]
24. Ladonin, D.V.; Mikhailova, A.P. Heavy metals and arsenic in soils and street dust of the South-Eastern administrative district: Results of multi-year research. *Eurasian Soil Sci.* **2020**, *11*, 1635–1644. [CrossRef]
25. Prokof'Eva, T.V.; Shoba, S.A.; Lysak, L.V.; Ivanova, A.E.; Glushakova, A.M.; Shishkov, V.A.; Lapygina, E.V.; Shilaika, P.D.; Glebova, A.A. Organic constituents and biota in the urban atmospheric solid aerosol: Potential effects on urban soils. *Eurasian Soil Sci.* **2021**, *54*, 1532–1545. [CrossRef]
26. MalAmiri, N.; Rashki, A.; Hosseinzadeh, S.R.; Kaskaoutis, D. Mineralogical, geochemical, and textural characteristics of soil and airborne samples during dust storms in Khuzestan, southwest Iran. *Chemosphere* **2022**, *286*, 131879. [CrossRef] [PubMed]
27. Awadh, S.M. Geochemistry and mineralogical composition of the airborne particles of sand dunes and dust storms settled in Iraq and their environmental impacts. *Environ. Earth Sci.* **2012**, *66*, 2247–2256. [CrossRef]
28. Urusevskaya, I.S.; Kolesnikova, V.M.; Vertyankina, V.Y. Anthropogenic soils on the territory of the New Jerusalem Monastery, Moscow region. *Eurasian Soil Sci.* **2018**, *51*, 1095–1104. [CrossRef]
29. Kolesnikova, V.M.; Urusevskaya, I.S.; Vertyankina, V.Y. Reflections on the modern soil cover of the New Jerusalem Monastery: The history of anthropogenic landscape transformation. In *Urbanization: Challenge and Opportunity for Soil Functions and Ecosystem Services*; Vasenev, V., Dovletyarova, E., Cheng, Z., Prokof'eva, T., Morel, J., Ananyeva, N., Eds.; SUITMA 2017; Springer Geography: New York, NY, USA, 2019; pp. 42–50. [CrossRef]
30. Filippova, O.I.; Kholodov, V.A.; Safronova, N.A.; Yudina, A.V.; Kulikova, N.A. Particle-Size, Microaggregate-Size, and Aggregate-Size Distributions in Humus Horizons of the Zonal Sequence of Soils in European Russia. *Eurasian Soil Sci.* **2019**, *52*, 300–312. [CrossRef]
31. Sileva, T.M.; Ivanov, V.V.; Shoba, S.A. Diagnostics of minerals of large fractions of soils. In *Student Book*; MAKS Press: Moscow, Russia, 2015; p. 80.
32. Shishov, V.L.; Voitovich, N.V. *Soils of the Moscow Region and Their Use*; Soil Dokuchaev in-t: Moscow, Russia, 2002; p. 500.
33. Suslova, E.G. Forests of the Moscow region. *Ecosyst. Ecol. Dyn.* **2019**, *1*, 1–72.
34. Urusevskaya, I.S.; Kolesnikova, V.M.; Timofeeva, A.S. Soils of the Istra valley within the New Jerusalem monastery and its surroundings. *Moscow Univ. Soil Sci. Bull.* **2015**, *70*, 153–160. [CrossRef]
35. Environmental Passport of the City of Istra. Available online: http://ecopassmo.mosreg.ru/media/region_doc/g_o_istra.pdf (accessed on 15 November 2021).
36. Elcheva, I.O.; Zubkova, V.M.; Gaponenko, A.V. Assessment of the level of soil pollution in the city of Istra. *Bull. Mosc. State Univ. Ser. Nat. Sci.* **2018**, *1*, 42–50.
37. Gradusov, B. P Granulo-Petrographic-Mineralogical Soil Discharges. National Atlas of Soils of the Russian Federation M: Astrel: AST, 2011.-Maps. Scale 1:30 000 000. 2011, 214–215. [In Russian]. Available online: https://soil-db.ru/soilatlas/razdel-5-pochvennyy-pokrov/granulo-petrografo-mineralogicheskie-razryady-pochv (accessed on 1 November 2021).
38. Coch, N.K.; Krinsley, D.H. Comparison of stratigraphic and electron microscopic studies in Virginia Pleistocene coastal sediments. *J. Geol.* **1971**, *79*, 426–437. [CrossRef]
39. Alekseeva, V.A. Movement and diagenetic transformation of quartz grains and their paleogeographic interpretation. *Vestn. MGU. Ser. 5. Geogr.* **2003**, *4*, 40–46.
40. Armstrong-Altrin, J.S.; Natalhy-Pineda, O. Microtextures of detrital sand grains from the Tecolutla, Nautla, and Veracruz beaches, western Gulf of Mexico, Mexico: Implications for depositional environment and paleoclimate. *Arab. J. Geosci.* **2014**, *7*, 4321–4333. [CrossRef]

41. Krinsley, D.H.; Doornkamp, J.C. *Atlas of Quartz Sand Surface Textures*; Cambridge University Press: Cambridge, UK, 1973; p. 53.
42. Ramos-Vazquez, M. Provenance and paleoenvironmental significance of microtextures in quartz and zircon grains from the Paseo del Mar and Bosque beaches, Gulf of Mexico. *J. Earth Syst. Sci.* **2020**, *129*, 225. [CrossRef]
43. Itamiya, H.; Sugita, R.; Sugai, T. Analysis of the surface microtextures and morphologies of beach quartz grains in Japan and implications for provenance research. *Prog. Earth Planet. Sci.* **2019**, *6*, 1–14. [CrossRef]
44. Shao, L.Y.; Li, Y.W.; Jones, T.; Santosh, M.; Liu, P.J.; Zhang, M.Y.; Xu, L.; Li, W.J.; Lu, J.; Yang, C.X.; et al. Airborne microplastics: A review of current perspectives and environmental implications. *J. Clean. Prod.* **2022**, *347*, 131048. [CrossRef]
45. Liu, P.; Shao, L.; Li, Y.; Jones, T.; Cao, Y.; Yang, C.-X.; Zhang, M.; Santosh, M.; Feng, X.; Bérubé, K. Microplastic atmospheric dustfall pollution in urban environment: Evidence from the types, distribution, and probable sources in Beijing, China. *Sci. Total Environ.* **2022**, *838*, 155989. [CrossRef]
46. He, Y.; Peng, C.; Zhang, Y.; Guo, Z.; Xiao, X.; Kong, L. Comparison of heavy metals in urban soil and dust in cities of China: Characteristics and health risks. *Int. J. Environ. Sci. Technol.* **2022**, *20*, 2247–2258. [CrossRef]
47. Muller, G. Index of geoaccumulation in sediments of the Rhine river. *Geo J.* **1969**, *2*, 108–118.
48. Taghavi, S.N.; Kamani, H.; Dehghani, M.H.; Nabizadeh, R.; Afshari, N.; Mahvi, A.H. Assessment of Heavy Metals in Street Dusts of Tehran Using Enrichment Factor and Geo-Accumulation Index. *Health Scope* **2019**, *8*, e57879. [CrossRef]
49. Kowalska, J.B.; Mazurek, R.; Gąsiorek, M.; Zaleski, T. Pollution indices as useful tools for the comprehensive evaluation of the degree of soil contamination–A review. *Environ. Geochem. Health* **2018**, *40*, 2395–2420. [CrossRef] [PubMed]
50. Khademi, H.; Gabarrón, M.; Abbaspour, A.; Martínez-Martínez, S.; Faz, A.; Acosta, J.A. Environmental impact assessment of industrial activities on heavy metals distribution in street dust and soil. *Chemosphere* **2019**, *217*, 695–705. [CrossRef] [PubMed]
51. Zhang, J.; Liu, C.L. Riverine Composition and Estuarine Geochemistry of Particulate Metals in China—Weathering Features, Anthropogenic Impact and Chemical Fluxes. *Estuar. Coast. Shelf Sci.* **2002**, *54*, 1051–1070. [CrossRef]